


RESEARCH ARTICLE - FUNDAMENTAL

Lateral induction limits the impact of cell connectivity on Notch signaling in arterial walls

Tommaso Ristori^{1,2,3}  | Oscar M. J. A. Stassen^{1,2} | Cecilia M. Sahlgren^{1,2,3} | Sandra Loerakker^{1,3}

¹Department of Biomedical Engineering, Eindhoven University of Technology, Eindhoven, The Netherlands

²Faculty of Science and Engineering, Biosciences, Åbo Academi University, Turku, Finland

³Institute for Complex Molecular Systems, Eindhoven University of Technology, Eindhoven, The Netherlands

Correspondence

Sandra Loerakker, Institute for Complex Molecular Systems, Eindhoven University of Technology, Eindhoven, The Netherlands.

Email: s.loerakker@tue.nl

Funding information

H2020 European Research Council, Grant/Award Numbers: 771168, 802967; Suomen Akatemia, Grant/Award Number: 218062

Abstract

It is well known that arteries grow and remodel in response to mechanical stimuli. Vascular smooth muscle cells are the main mediators of this process, as they can switch phenotype from contractile to synthetic, and vice-versa, based on the surrounding bio-chemo-mechanical stimuli. A correct regulation of this phenotypic switch is fundamental to obtain and maintain arterial homeostasis. Notch, a mechanosensitive signaling pathway, is one of the main regulators of the vascular smooth muscle cell phenotype. Therefore, understanding Notch dynamics is key to elucidate arterial growth, remodeling, and mechanobiology. We have recently developed a one-dimensional agent-based model to investigate Notch signaling in arteries. However, due to its one-dimensional formulation, the model cannot be adopted to study complex non-symmetrical geometries and, importantly, it cannot capture the realistic “cell connectivity” in arteries, here defined as the number of cell neighbors. Notch functions via direct cell-cell contact; thus, the number of cell neighbors could be an essential feature of Notch dynamics. Here, we extended the agent-based model to a two-dimensional formulation, to investigate the effects of cell connectivity on Notch dynamics and cell phenotypes in arteries. The computational results, supported by a sensitivity analysis, indicate that cell connectivity has marginal effects when Notch dynamics is dominated by the process of lateral induction, which induces all cells to have a uniform phenotype. When lateral induction is weaker, cells exhibit a nonuniform phenotype distribution and the percentage of synthetic cells within an artery depends on the number of neighbors.

KEYWORDS

agent-based model, artery, growth and remodeling, jagged, lateral induction, notch signaling

Abbreviations: 1D, one-dimensional; 2D, two-dimensional; IMT, intima-media thickness; MSE, mean squared error; NICD, Notch-IntraCellular Domain; STD, standard deviation; VSMCs, Vascular Smooth Muscle Cells.

This is an open access article under the terms of the Creative Commons Attribution-NonCommercial-NoDerivs License, which permits use and distribution in any medium, provided the original work is properly cited, the use is non-commercial and no modifications or adaptations are made.

© 2020 The Authors. *International Journal for Numerical Methods in Biomedical Engineering* published by John Wiley & Sons Ltd.

1 | INTRODUCTION

Arteries accommodate their morphology and composition in response to changes in the surrounding mechanical stimuli. For example, prolonged hypertension can cause arterial wall thickening and variation of the residual stress.¹⁻⁴ Similarly, the remodeling and organization of several arterial components, such as collagen fibers, is highly influenced by mechanical factors.^{5,6} Although numerous studies have proposed that arteries grow and remodel to maintain homeostatic levels of mechanical parameters, for example, wall shear stress and circumferential stress (see Humphrey et al⁷ for a review), the underlying mechanisms are still insufficiently understood. An improved mechanistic understanding could not only potentiate the development of novel treatments for arterial diseases but also facilitate the design of tissue-engineered vascular grafts.

Vascular smooth muscle cells (VSMCs) populating the vessel wall are the main mediators of arterial growth and remodeling. Importantly, these cells exhibit a unique plasticity in terms of their phenotypes, known as synthetic and contractile. Synthetic VSMCs show high levels of proliferation, migration, and extracellular matrix synthesis, while contractile VSMCs exhibit higher levels of contractility.^{8,9} While synthetic VSMCs play a fundamental role during blood vessel development, contractile VSMCs are essential to regulate the vascular tone in fully grown healthy arteries. In the case of disease or upon injury,¹⁰⁻¹² contractile VSMCs can switch phenotype and become synthetic, thereby changing their behavior and contributing to the morphological changes of the artery. Elucidating the stimuli regulating the switch between contractile and synthetic VSMCs is therefore fundamental for understanding arterial growth and remodeling in health and disease.

Notch signaling is one of the key players in the context of VSMC phenotype regulation. Notch is an evolutionary conserved cell-cell signaling pathway that is crucial for the development and homeostasis of many human tissues. VSMCs are known to express three Notch receptors (Notch1, Notch2, and Notch3)^{13,14} and three Notch ligands (Jagged1, Jagged2, and Delta-like ligand1, Dll1).^{14,15} Activation of these Notch receptors by Notch ligands present on the membrane of neighboring cells leads to translocation of the Notch-IntraCellular domain (NICD) to the cell nucleus of the receiving cell, which subsequently influences gene expression and thus production of proteins, including Notch receptors and ligands. Notch activation is often assumed to induce downregulation of Delta-like ligands and upregulation of Jagged ligands.^{16,17} For this reason, Delta-like ligands are usually associated with lateral inhibition processes giving rise to cell populations with alternating phenotypes, while Jagged ligands are associated with lateral induction processes that enable a transmission of Notch transactivation to cells located further away from cells originally initiating the signal.¹⁸ In vivo studies have shown that VSMCs mainly express Jagged1.¹⁹ Moreover, in one of our previous studies,²⁰ we have detected very limited expression of Dll1 in VSMCs in vitro, compared to Jagged1 expression. Therefore, the process of lateral induction is most likely dominant for this type of cells. In VSMCs, Notch3 activation by Jagged1 upregulates not only the production of Notch3 and Jagged1^{18,21} but also the presence of proteins associated with cellular contractile features, such as α -smooth muscle actin.^{18,21,22} For this reason, Notch activation has been linked to the phenotypic switch from synthetic to contractile VSMCs. In vitro experiments have also shown that VSMCs downregulate Notch3 and Jagged1 levels in response to cyclic strain.^{20,23} Together, the influence of Notch on VSMC differentiation and the mechanosensitivity of this signaling pathway might contribute to the effects of mechanical stimuli on VSMC behavior²³⁻²⁶ and could therefore be strongly linked to the regulation of arterial growth, remodeling, and homeostasis (Figure 1A).

Recently, we have highlighted the potential importance of Notch signaling for arterial homeostasis.²⁰ This was achieved with an agent-based model for Notch signaling built on previous seminal studies,^{16,17,27} incorporating both the effects of mechanics on Notch protein levels and the influence of Notch activation on VSMC phenotype.²⁰ A scheme of the main assumptions of the computational model for Notch signaling among VSMCs is shown in Figure 1A. The computational results showed that Notch mechanosensitivity induces a collective phenotypic switch of VSMCs from synthetic for relatively thin arteries, to contractile for larger arteries. Interestingly, the model also predicted this switch to correspond approximately with the homeostatic arterial wall thickness observed in human arteries. However, some limitations of the computational model still need to be addressed. In fact, in that previous study,²⁰ due to the axial symmetry and periodicity of arteries, a one-dimensional (1D) model analyzing Notch signaling among transmurally distributed VSMCs was adopted. Although advantageous in terms of computational costs and simplicity, this 1D approach cannot capture the actual “cell connectivity” of cells in arteries, here defined as the number of cell neighbors. Notch signaling pathway functions via direct cell-cell contacts (juxtacrine signaling); therefore, cell connectivity is potentially a very influential parameter for the Notch signaling dynamics.

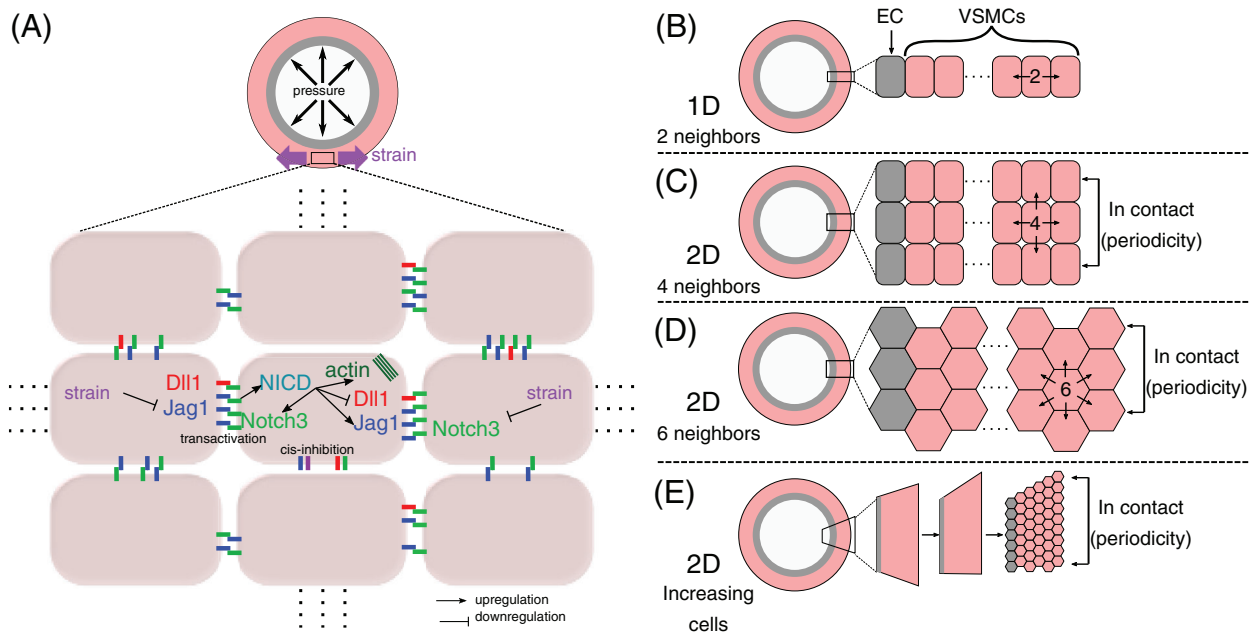


FIGURE 1 Scheme of the computational model for Notch signaling (A) and the different model formulations (B-E). A, Scheme showing the main assumptions of the computational model for Notch signaling among Vascular Smooth Muscle Cells. In the model, more specifically, transactivation of Notch3 by the ligands leads to upregulation of Notch3, Jagged1, and cellular contractile properties. On the other hand, Notch3 transactivation downregulates Dll1, while the strain experienced by cells (caused by blood pressure) causes downregulation of Jagged1 and Notch3. B-E, In the 1D agent-based model, all cells have a maximum of two neighbors. For 2D simulations with a squared lattice, all cells have a maximum of four neighbors, while a hexagonal lattice corresponds to six neighbors. Finally, we depict a scheme leading to the simulations of arteries with an increasing number of cells along the circumferential direction, going from the inner to the outer layer of the arterial wall

Here, we thus extended the previous 1D agent-based model for Notch signaling in arteries to a two-dimensional (2D) formulation, enabling the investigation of the effects of cell connectivity on the dynamics of Notch signaling and VSMC phenotypes in arteries. In particular, we analyzed Notch signaling for VSMCs having from 2 to 6 cell neighbors. The computational results of the 1D and 2D formulations were compared by using the original parameters and by performing a sensitivity analysis.

2 | METHODS

In what follows, the main features of the 2D agent-based model for Notch signaling are summarized, highlighting the differences with the 1D formulation.²⁰

2.1 | 2D agent-based model for Notch signaling

Built upon previous studies,^{16,17,20,27,28} the agent-based model describes Notch signaling among cells in arteries by accounting for the transactivation of Notch3 (N) by Jagged1 (J) or Dll1 (D) present on the membrane of neighboring cells. Notch transactivation leads to an increase of NICD (I), with consequential effects on the production of the Notch proteins N , J , and D , which were analyzed for each single VSMC. In Loerakker et al.,²⁰ each single cell was indicated with the index i , such that N_i , J_i , D_i , and I_i are the Notch protein levels in the cellular layer $i \in \mathbb{N}$, with the cells transversally distributed along a single line through the arterial wall (Figure 1B). Here, to extend the model to a 2D formulation, we added the index $j \in \mathbb{N}$ to indicate the circumferential position of the cell in the arterial wall. To distinguish among the cells distributed along the 2 directions in 2D, in what follows, we refer to “row” to indicate a line of cells distributed along the radial direction and we refer to “column” or “layer” to indicate a line of cells distributed along the circumferential direction (Figure 1C-E). Therefore, the subscript ij refers to the cell located in the i -th column and j -th

row. The variation over time t of the Notch proteins N_{ij} , J_{ij} , D_{ij} , and I_{ij} was described by the following ordinary differential equations:

$$\frac{dN_{ij}}{dt} = N_{\text{pr,mech}} H^s(I_{ij}, \lambda_N, n_N) - \frac{M}{M_{ij}} N_{ij} \left[k_c (D_{ij} + J_{ij}) + k_t \sum_{k=1}^{M_{ij}} \frac{D_{k,ij} + J_{k,ij}}{M_{k,ij}} \right] - \gamma N_{ij}, \quad (1)$$

$$\frac{dJ_{ij}}{dt} = J_{\text{pr,mech}} H^s(I_{ij}, \lambda_J, n_J) - \frac{M}{M_{ij}} J_{ij} \left[k_c N_{ij} + k_t \sum_{k=1}^{M_{ij}} \frac{N_{k,ij}}{M_{k,ij}} \right] - \gamma J_{ij}, \quad (2)$$

$$\frac{dD_{ij}}{dt} = D_{\text{pr}} H^s(I_{ij}, \lambda_D, n_D) - \frac{M}{M_{ij}} D_{ij} \left[k_c N_{ij} + k_t \sum_{k=1}^{M_{ij}} \frac{N_{k,ij}}{M_{k,ij}} \right] - \gamma D_{ij}, \quad (3)$$

$$\frac{dI_{ij}}{dt} = \frac{M}{M_{ij}} N_{ij} k_t \sum_{k=1}^{M_{ij}} \frac{D_{k,ij} + J_{k,ij}}{M_{k,ij}} - \gamma_I I_{ij}. \quad (4)$$

Here, $N_{\text{pr,mech}}$, $J_{\text{pr,mech}}$, and D_{pr} label the production rate of the different Notch proteins; k_c and k_t , respectively, scale the cis-inhibition and transactivation rate of Notch ligands with Notch receptors; M is the typical number of cell neighbors of VSMCs, M_{ij} is the number of neighbors of the cell ij , while $M_{k,ij}$ is the number of neighbors of the neighbor number k of the cell ij , with k auxiliary index. Similarly, $N_{k,ij}$, $J_{k,ij}$, and $D_{k,ij}$ are the Notch proteins present in the neighbor number k of the cell ij (the external Notch proteins available for binding). Finally, γ and γ_I are the degradation rates of the Notch proteins and NICD, respectively. H^s is a shifted Hill-type function describing the influence of the NICD level I on the production of Notch proteins:

$$H^s(I, \lambda, n) = \lambda + \frac{1 - \lambda}{1 + \left(\frac{I}{I_0}\right)^n}, \quad (5)$$

where n represents the sensitivity of the Notch protein production rate to the NICD level, while I_0 is the transition point of the Hill-type function from convex to concave. The parameter λ determines the effect of Notch activation on protein production (upregulation for $\lambda > 1$, downregulation for $0 < \lambda < 1$, and no effects when $\lambda = 1$). Furthermore, as fitted from in vitro experiments,²⁰ the production of Notch3 and Jagged1 was assumed to be downregulated by cyclic strain with an exponential fashion:

$$N_{\text{pr,mech}} = N_{\text{pr}} \exp(A_N \varepsilon); J_{\text{pr,mech}} = J_{\text{pr}} \exp(A_J \varepsilon). \quad (6)$$

Here, A_N and A_J quantify the downregulation of Notch3 and Jagged1 production in response to the strain ε experienced by cells in the arterial wall, while N_{pr} and J_{pr} indicate the protein production rates when no strain is applied. The strain experienced by cells in the arterial wall was approximated as

$$\varepsilon = \varepsilon_p \frac{\sigma_\theta}{\sigma_p}, \quad (7)$$

where ε_p and σ_p are the average physiological in vivo strain and stress, respectively, which are scaled with the average circumferential stress σ_θ in the modeled arterial wall. This last term was approximated with the Laplace's law, such that $\sigma_\theta = rp/h$, where p indicates the blood pressure, r the arterial internal radius, and h the wall thickness. This last term was computed by assuming that each cell layer is 0.01 mm thick.

For a complete description of the derivation of Equations (1) to (4) from an approach similar to Shaya et al,²⁸ we refer the reader to the Appendix. We observe that these equations are a generalization of the equations adopted in Boareto et al¹⁷ and Loerakker et al.²⁰ The major difference is represented by the inclusion of the factor $\frac{M}{M_{ij}}$, which multiplies both the cis-inhibition and transactivation terms. This scaling factor accounts for the effects that having different

numbers of neighbors causes on the distribution of Notch proteins within a cell and, therefore, on the likelihood of both cis-inhibition and transactivation events. In particular, assuming that cells equally distribute their Notch proteins at the interface with their neighbors, cells with different numbers of neighbors also have a different density of both receptors and ligands at these interfaces, even when they have equal values of total Notch protein content and, consequently, they have a different likelihood to experience cis-inhibition and transactivation events. Importantly, when VSMCs within a cell population always have two neighbors (such as for 1D simulations, Figure 1B), $\frac{M}{M_{ij}} = 1$ and Equations (1) to (4) become the same as the equations proposed in the studies of Boareto et al.¹⁷ and Loerakker et al.²⁰ Nevertheless, compared to Loerakker et al.,²⁰ we did not include Jagged polarized clustering, which refers to the localization of Jagged1 proteins only on the side of VSMCs facing the outer side of the arterial wall. In the previous model formulation, this had little effects; therefore, for simplicity, Jagged polarized clustering was here neglected.

2.2 | Boundary/initial conditions and numerical implementation

In addition to VSMCs, similar to Loerakker et al.,²⁰ endothelial cells were considered in the model by assuming that the first layer of VSMCs is in contact with a layer of endothelial cells present on the luminal side (Figure 1C-E). Endothelial cells were assumed to express a constant value of Jagged J_{EC} , while other Notch proteins were neglected.

When simulating Notch signaling with the 2D formulation, to limit the computational costs, 10 cell rows were considered. Due to the axial symmetry of arteries, the first row of cells was assumed to be in contact with the last row, consistent with periodic boundary conditions (Figure 1).

As in Loerakker et al.²⁰ all simulations were repeated 25 times with different initial conditions of the unknown variables of Equations (1) to (4), thereby randomly choosing the values of $N_{ij}(0)$, $J_{ij}(0)$, and $D_{ij}(0)$ between 0 and 6000 molecules, and the value of $I_{ij}(0)$ between 0 and 600 molecules for each ij cell considered. The computational results did not change significantly when the simulations were repeated 100 times.

The differential equations were solved with an explicit scheme (time-step $t = 0.01$ hour) until $t > 250$ hours and until convergence, here identified as the minimum time such that $\frac{1}{K} \sum_{i,j} \left| \frac{dI_{ij}}{dt}(t) \right| < 10^{-2}$, with K the total number of cells considered.

Once convergence was reached, a specific phenotype was assigned to each VSMC based on their value of I_{ij} : VSMCs with $0 < I_{ij} < 100$ were classified as synthetic (or Sender), while VSMCs with $100 \leq I_{ij} < 300$ were identified as contractile (or Sender/Receiver). As in Loerakker et al.,²⁰ a specific phenotype was not assigned for VSMCs with $I_{ij} \geq 300$, which were just referred to as Receiver cells.

The same parameters as in Loerakker et al.²⁰ were considered in the simulations. In that study, arteries at different locations of the arterial tree were simulated. As the focus of the present study is on the influence of the number of cell neighbors on Notch signaling in arteries, only the carotid artery of young individuals was here simulated as a representative artery. An overview of the original model parameters can be found in Table 1, and a discussion of these parameters can be found in the Appendix B. For the sensitivity analysis of the results, these model parameters were varied one by one, with parameter variations going from -75% to $+75\%$ of the original value.

For each parameter set, Notch signaling was simulated for arteries having a different number of cell layers, going from 1 to 100 layers, corresponding to values of intima-media thickness (IMT) going from 0.01 to 1 mm. We observe here that muscular arteries also contain a fibrosa layer (such that the total arterial wall thickness is the sum between the IMT and the fibrosa thicknesses). Nevertheless, the fibrosa is mostly composed by collagenous fibers and sparsely distributed fibroblasts. Therefore, this layer was excluded from our analysis centered on cell-cell signaling among VSMCs and, given its relatively small thickness in muscular arteries, we assumed that the arterial stress could be reasonably estimated from the blood pressure, luminal radius, and IMT.

3 | RESULTS

3.1 | 1D and 2D simulations exhibit similar trends also when neglecting periodicity

To get an initial understanding of the computational results deriving from the 2D formulation, we ran simulations by assuming that all VSMCs, except for cells in the first/last rows and columns, have four neighbors (corresponding to a

Parameter	Value	Description
N_{pr}	1400 h ⁻¹	Notch3 baseline production
D_{pr}	100 h ⁻¹	Dll1 baseline production
J_{pr}	1600 h ⁻¹	Jagged1 baseline production
J_{EC}	4000	Constant Jagged1 content in ECs
k_c	5 × 10 ⁻⁴ h ⁻¹	cis-inhibition rate
k_t	2.5 × 10 ⁻⁵ h ⁻¹	transactivation rate
γ	0.1 h ⁻¹	Notch protein degradation rate
γ_I	0.5 h ⁻¹	NICD degradation rate
λ_N	2.0	Effect of transactivation on Notch3 production
λ_D	0.0	Effect of transactivation on Dll1 production
λ_J	2.0	Effect of transactivation on Jagged1 production
n_N	2.0	Sensitivity of Notch3 production to transactivation
n_D	2.0	Sensitivity of Dll1 production to transactivation
n_J	5.0	Sensitivity of Jagged1 production to transactivation
I_0	200	Transition point of shifted Hill-type function H^s
A_N	-5.79	Sensitivity of Notch3 production to strain
A_J	-4.17	Sensitivity of Jagged1 production to strain
ϵ_p	0.075	Average physiological in vivo strain
σ_p	107 mmHg	Average physiological in vivo stress
p	16 kPa	Maximum systolic blood pressure
r	3.2 mm	Internal radius of young carotid arteries

TABLE 1 Model parameters for original simulations

Abbreviation: NICD, Notch IntraCellular Domain.

squared lattice). At first, no periodic boundary conditions for the first and last rows of cells were considered (Figure 1C, without periodicity). In particular, in this case, it was assumed that cells at the boundaries are next to cells with no viable Notch proteins or only extracellular matrix. As shown in Figure 2, with these conditions, the trends observed for the 1D and 2D simulations are similar, but quantitative differences can be observed. In particular, both in 1D and 2D, all VSMCs are synthetic for relatively small arteries (Figure 2B) and exhibit very low levels of Jagged, Notch, and NICD, while the levels of Delta are high (Figure 2C-F). The levels of Notch and NICD increase upon increasing the arterial wall thickness, until almost all VSMCs become contractile (or Sender/Receiver). While this phenotypic switch is approximately collective for 1D simulations, for which the vast majority of VSMCs become contractile, 2D simulations without periodic boundary conditions predict that approximately 20% of VSMCs remain synthetic. We observe that this value depends on the number of rows considered; for example, approximately 35% of cells remain synthetic if six rows are considered. As shown in Figure 2A, the cells that remain synthetic correspond to the VSMCs present at the boundaries of the squared lattice, thereby suggesting that boundary effects are present. This can be explained as follows: VSMCs present on the first/last rows or last column of the lattice have only three cell neighbors; consequently, they are not in contact with enough Notch ligands, their Notch transactivation remains low (as their NICD value), and they are therefore predicted as being synthetic.

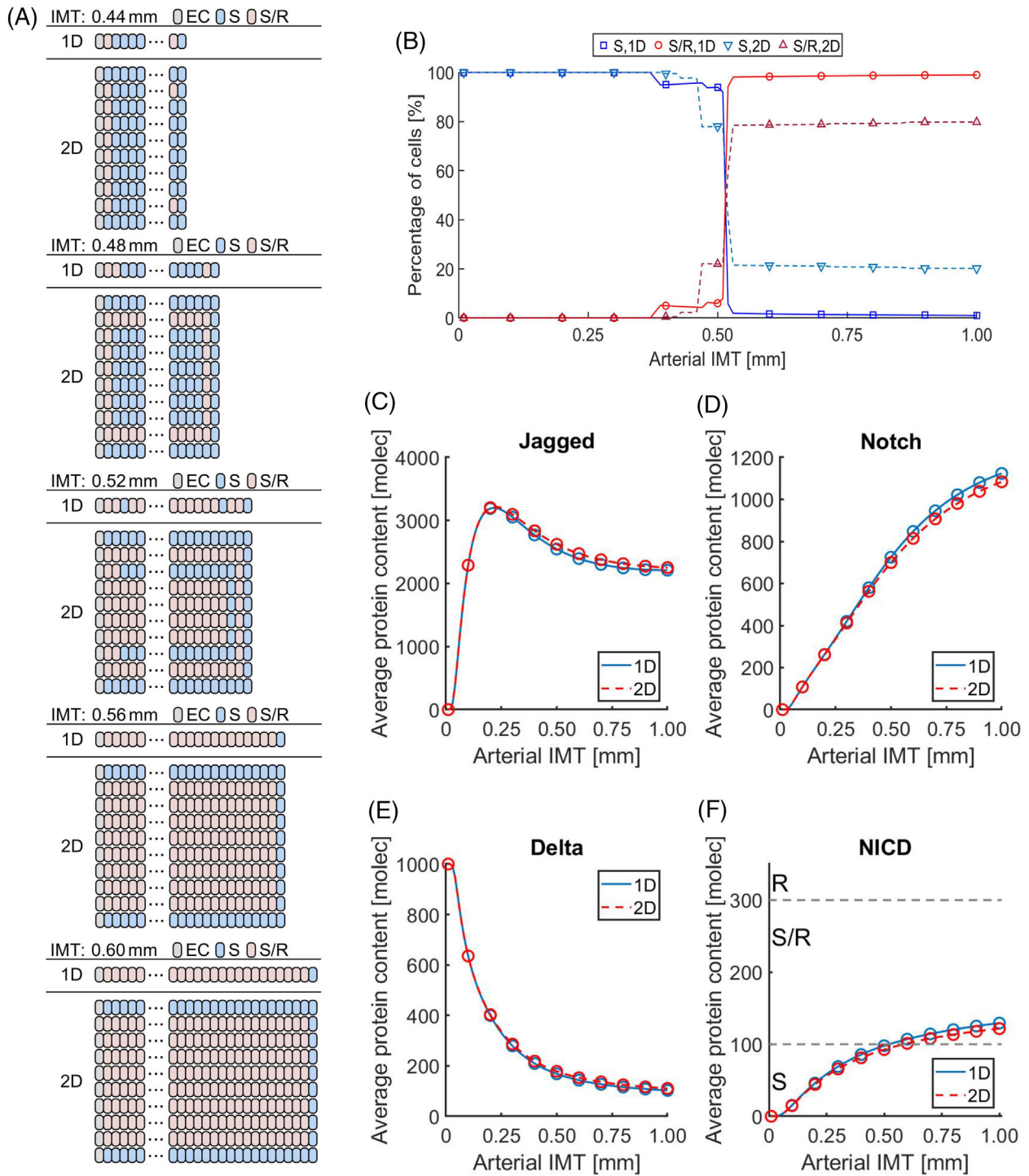


FIGURE 2 1D and 2D simulations with four neighbors per cell, without periodic boundary conditions, differ because of boundary effects. A, Example of computational results for one specific set of initial conditions, for values close to the transition thickness. Gray cells are endothelial cells, blue cells are synthetic (or Sender), while red cells are contractile (or Sender/Receiver). The 2D results are similar to the 1D results, despite differences that can be observed for the first and last three rows of cells. B, Percentage of synthetic (S) and contractile (S/R) Vascular Smooth Muscle Cells (VSMCs) for arteries of different intima-media thickness (IMT). 1D simulations exhibit an almost collective phenotypic switch of VSMCs for the IMT approximately equal to 0.50 mm. For 2D simulations, the switch is not collective anymore. C-F, Values of Jagged (C), Notch (D), Delta (E), and NICD (F) for arteries of different IMT, averaged over all VSMCs, such that each point on the horizontal axis refers to simulations of arteries with different IMT. 1D and 2D simulations present similar trends but predict slightly different values of Notch proteins, particularly at high wall thicknesses

3.2 | Jagged-Notch lateral induction limits the impact of cell connectivity on Notch dynamics

The results of the 1D simulations are almost exactly the same as the results obtained with the 2D formulation when the periodic boundary conditions are included (Figure 3). In this formulation, the VSMCs belonging to the first row are connected with VSMCs present in the last row (Figure 1B). As a consequence of the periodic boundary conditions, also the cells at the boundaries have four neighbors (as the vast majority of VSMCs) and therefore they receive enough signal from their neighbors to become contractile cells when the transition thickness is reached. Consequently, in this case, a collective switch from synthetic VSMCs for small arterial walls to contractile VSMCs for larger arterial walls can be observed for both 1D and 2D (Figure 3A,B), which exhibit almost identical results in terms of the average values of Jagged, Notch, Delta, and NICD (Figure 3C-F). Small differences can be observed only when looking at the percentage of contractile or synthetic VSMCs for arterial wall thicknesses slightly smaller than the transition level (Figure 3A,B). These differences are most likely due to the choice of a sharp transition level of NICD discriminating between synthetic and contractile cells, as in previous studies.^{17,20} In particular, according to the current model assumptions, when the NICD levels are close to the discriminating value, very small variations in the NICD value can give rise to larger differences concerning the assigned VSMC phenotype.

The same conclusions can be drawn when simulating arteries populated by VSMCs having six neighbors each (Figure 1C), with periodic boundary conditions (Figure 4). The 1D and 2D results are extremely similar, and small differences can be seen only when analyzing the percentage of synthetic and contractile VSMCs with arterial wall thicknesses that are close to the transition level. The equivalence of the 1D and 2D simulations that appears independent of the number of neighbors is most likely due to Jagged-Notch lateral induction. In particular, in the model, Notch transactivation in one VSMC leads to an upregulation of both Notch and Jagged in that cell, which can then efficiently transactivate neighboring cells giving rise to a feedback loop that induces cells to have a uniform value of NICD. Since VSMCs mainly express Jagged1 as Notch ligand, we chose $D_{pr} \ll J_{pr}$, which causes the lateral inhibition as induced by Delta-Notch signaling to have little effects in our simulations compared to lateral induction. Therefore, for these simulations, all cells were induced to have a similar amount of NICD, irrespective of the number of cell neighbors (when this number is constant throughout the cell population).

3.3 | Cell connectivity affects Notch dynamics when Jagged-Notch lateral induction is perturbed

Next, we aimed at elucidating whether the equivalence between simulations with VSMCs having a different number of neighbors is a consequence of the strong effects of lateral induction and the chosen model parameters. To this aim, we performed a sensitivity analysis, running simulations by varying the model parameters one by one, with parameter variations going from -75% to $+75\%$ of the original parameter values. In Figure 5, for each parameter variation, we show the mean squared error (MSE) resulting from the comparison of the percentage of synthetic VSMCs for arterial wall thicknesses going from 0.01 to 1 mm, predicted with the simulations adopting different formulations:

$$\text{MSE} = \frac{1}{100} \sum_{h=1}^{100} (P_{h,\hat{m}}^S - P_{h,m}^S)^2 \quad (8)$$

where $P_{h,\hat{m}}^S$ and $P_{h,m}^S$ represent the percentage of synthetic cells predicted by the simulations for an artery with h layers of cells ($\text{IMT} = h \cdot 0.01$ mm), with a cell population having the number of cell neighbors uniform and equal to \hat{m} and m , respectively. Different subscripts \hat{m} and m were adopted to indicate that the MSE was computed between simulations assuming different numbers of neighbors, with $\hat{m}, m \in \{2, 4, 6\}$ and $\hat{m} \neq m$.

Except for a few parameter sets, the MSE obtained with different parameter values generally remained comparable to the MSE obtained with the original parameter values, indicated with a horizontal dashed line (Figure 5). Still, very large values of MSE were observed when varying the parameters λ_N , λ_J , and n_J , especially for simulations with six neighbors (Figure 5B,C). Interestingly, variations of these parameters also correspond to large values of the mean standard deviation of the percentage of synthetic VSMCs with respect to the initial conditions (Figure 6). Therefore, the

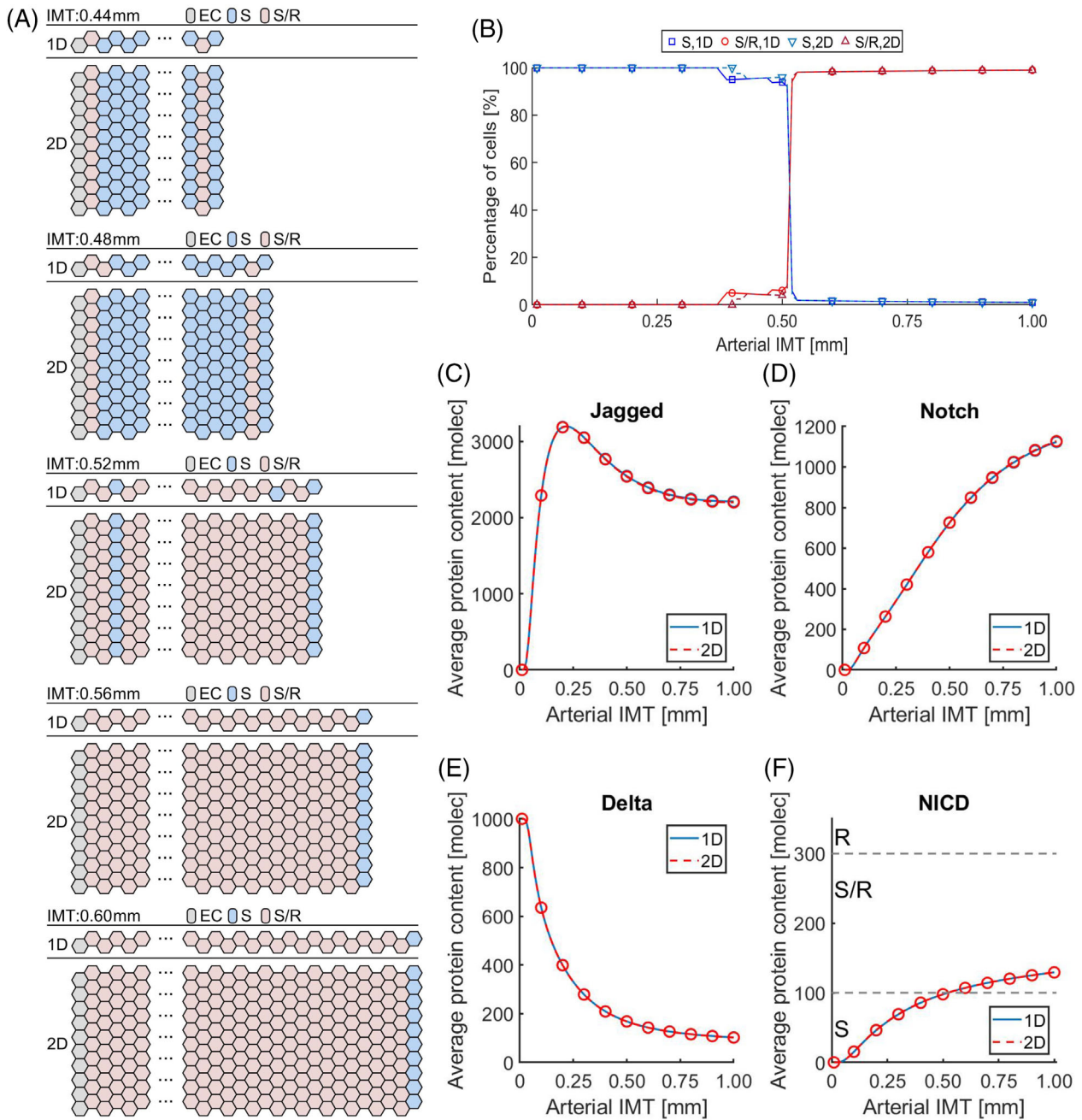
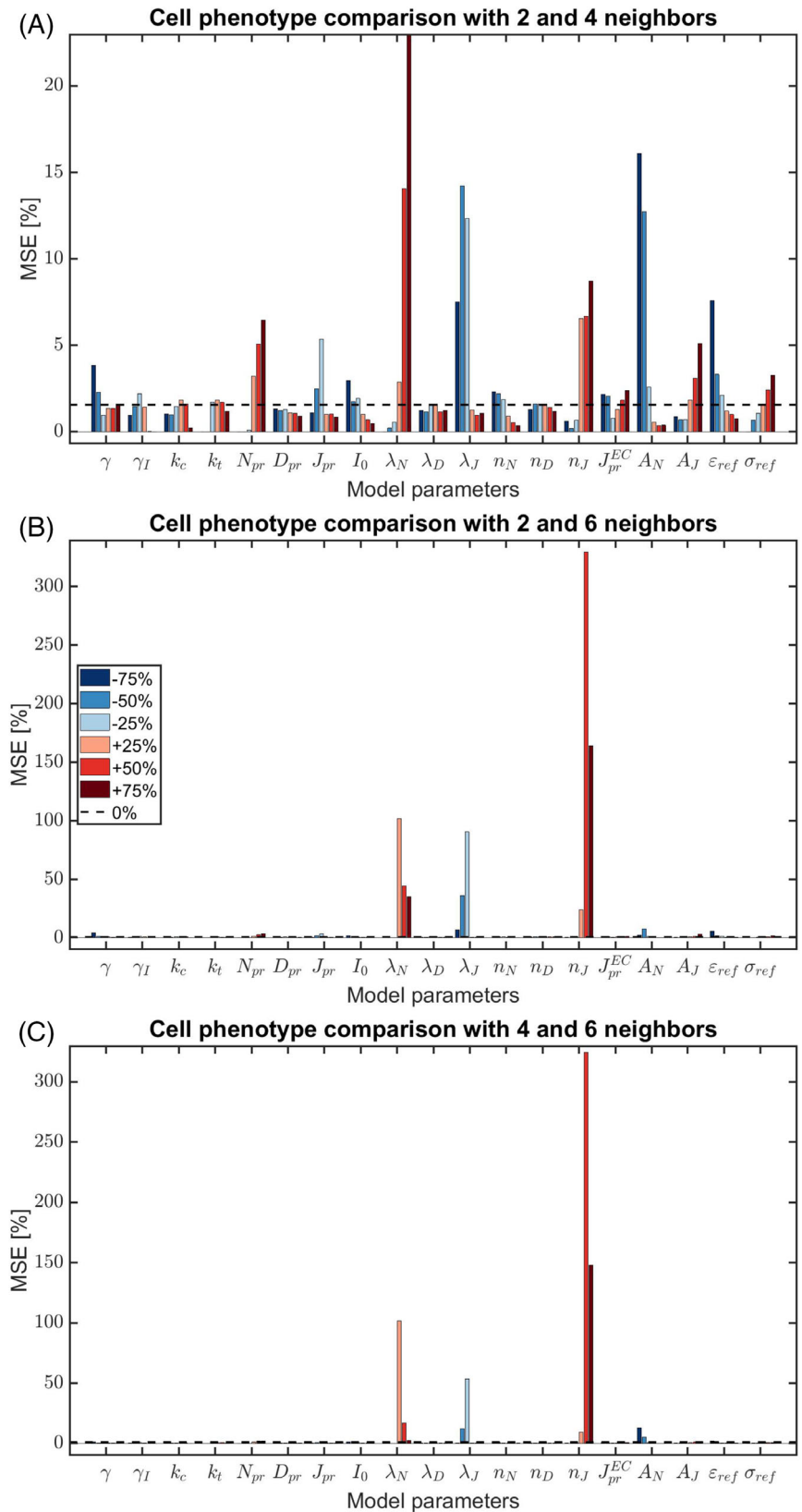


FIGURE 4 1D and 2D simulations with six neighbors per cell, considering periodic boundary conditions, present almost equal results. A, Example of computational results for one specific set of initial conditions, for values close to the transition thickness. The 1D and 2D results are approximately equivalent for these results, as well as for the percentage of synthetic (S) and contractile (S/R) Vascular Smooth Muscle Cells in arteries with different thickness (B) and for the average values of Notch proteins for arteries of different intima-media thickness (C-F)

The parameters λ_N , λ_J , and n_J are all related to the function H^s (Equation [5]), describing the effects of Notch transactivation (with the subsequent increase of NICD levels) on the production of Notch (λ_N) and Jagged (λ_J and n_J). When $H^s > 1$, Notch transactivation leads to upregulation of the different Notch proteins (depending on the production term that it multiplies in Equations [1]-[4]); when $H^s < 1$, Notch transactivation leads to downregulation; and for $H^s = 1$, Notch transactivation has no effects on Notch protein production. We observe that the simulations predict that cells have values of I below 200 (see eg, Figures 2-4F). As shown in Figure 7, for these values of I , the parameter variations correlated with large differences between the 1D and 2D simulations cause an increase of the Notch upregulation (Figure 7A) or a decrease of the Jagged upregulation (Figure 7B,C) as a result of Notch transactivation. It appears that

FIGURE 5 Some parameter variations cause large differences between 1D and 2D simulations. The figures show the mean squared error of the percentage of synthetic cells as computed by the 1D simulations against the 2D simulations with four (A) and six neighbors (B), or as computed by the 2D simulations with four neighbors against the 2D simulations with six neighbors (C). The color scheme represents model parameter variations (horizontal axis) going from negative (from -75% dark blue to -25% light blue) to positive ($+25\%$ light red to $+75\%$ dark red), and the horizontal dashed lines indicate the values resulting from the simulations with the original parameters



these parameter variations disrupt the process of Jagged-Notch lateral induction, which cannot induce a uniform level of NICD among the VSMCs anymore, and a scattered phenotypic pattern is present within the arterial wall (Figure 8). In particular, the decrease of Jagged upregulation weakens the process of Jagged-Notch lateral induction because, with these parameters, VSMCs with transactivated Notch mainly upregulate Notch while keeping Jagged approximately

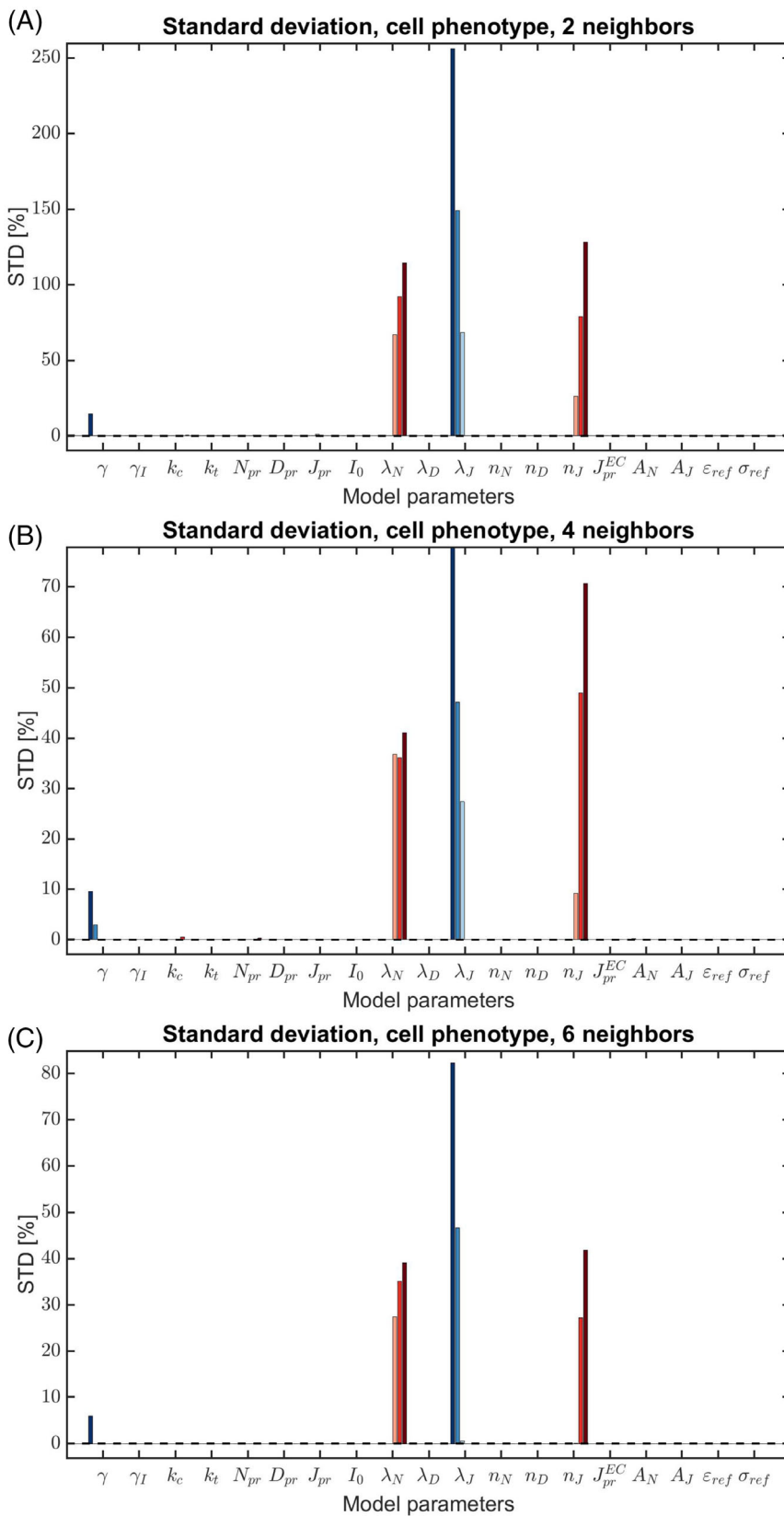


FIGURE 6 Some parameter variations cause large dependence of the computational results on the initial conditions. The figures show standard deviation of the percentage of synthetic cells within the same arterial wall with respect to different initial conditions. The color scheme represents model parameter variations (horizontal axis) going from negative (from -75% dark blue to -25% light blue) to positive (+25% light red to +75% dark red), and the horizontal dashed lines indicate the values resulting from the simulations with the original parameters

constant. Therefore, these cells rapidly become contractile cells because of high Notch transactivation but, on the other hand, due to their relatively low level of Jagged, they cannot induce the surrounding cells to become contractile via transactivation. This causes a major dependence of the simulations on the initial conditions (Figure 6) and on the

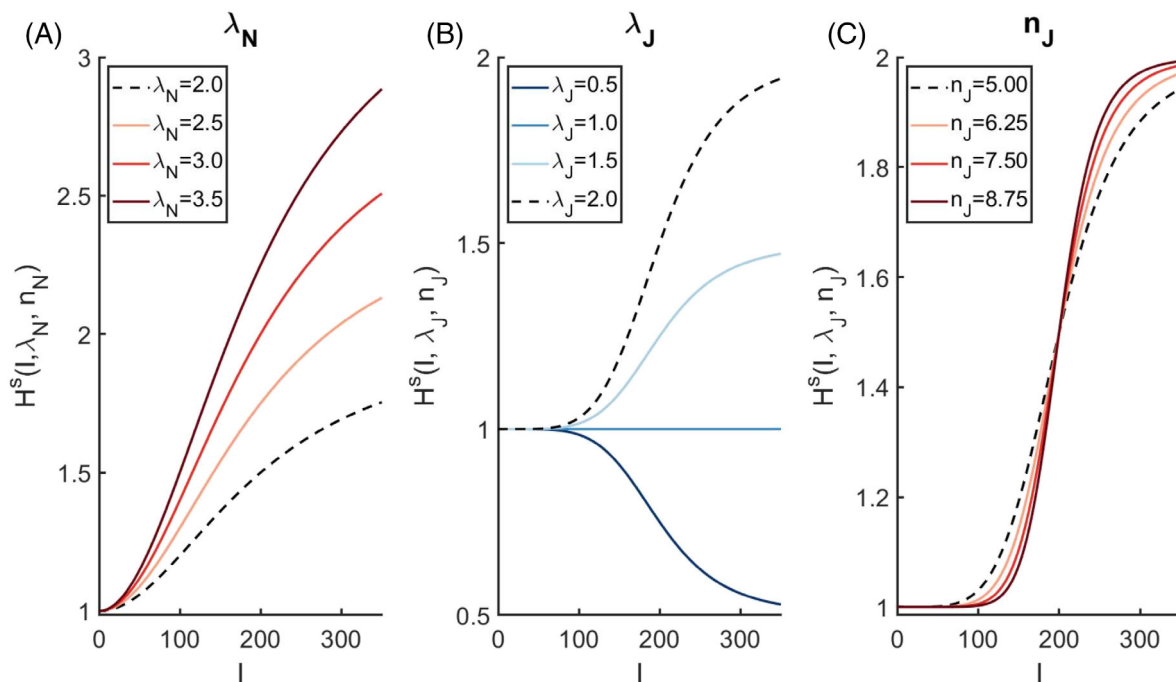


FIGURE 7 Shape of the shifted Hill-type function $H^s(I, \lambda, n)$ (Equation [5]) with parameter variations of λ_N (A), λ_J (B), and n_J (C). The values of H^s increase (A) or decrease (B) together with the values of λ_N (A) and λ_J (B). On the other hand, an inverse proportionality can be observed for variations of n_J (C) when $I < 200$, such that $H^s(I, \lambda_J, n_J)$ decreases for increasing values of n_J

number of cell neighbors (Figure 5). A similar mechanism seems to occur also when increasing Notch upregulation as a result of Notch transactivation (Figures 7A and 8), which also causes the solution to be more dependent on the initial conditions and on the number of neighbors (Figures 5 and 6). Therefore, it appears that, for an efficient Notch-Jagged lateral induction process, a correct balance between Notch and Jagged upregulation is necessary. This highlights the importance of determining the effects of Notch transactivation on Notch expression not only qualitatively but also quantitatively.

3.4 | Local variations of cell connectivity corresponds to local effects on Notch signaling

So far, all simulations were performed by assuming a constant number of VSMCs along the circumferential direction and a homogeneous cell distribution. However, small heterogeneities in the cell distribution might appear. These variations might be caused for example by the arterial geometry, as the arterial inner layer is shorter than the outer layer (Figure 1D), which can cause the number of cells along the circumferential direction increases when going from the inner to the outer arterial wall layers (Figure 1D). To investigate whether small heterogeneities in the cell distribution can potentially affect Notch dynamics in arteries, as a representative case, we assumed that the number of VSMCs present along the circumferential direction of the simulated arterial wall portion increases by one cell every three layers in the radial direction. This rate of increase was chosen to test the effects of a relatively high rate, while limiting the computational costs deriving from choosing higher rates. Periodic boundary conditions were adopted also in these simulations, by assuming that the first row of cells is connected with the last row of cells. We observe that, although the computational model was obtained by accounting for the length of the interfaces among cells (Appendix A), for simplicity in these latter simulations the length of the interfaces among cells was not considered. Nevertheless, Equations (1) to (4) are still valid by assuming that cells equally distribute their Notch proteins among their neighbors, irrespective of the length of the interfaces. This assumption enabled us to focus on the effects of variations in the number of neighbors rather than the cellular geometry, which can be much more variable. Therefore, the periodic boundary conditions were implemented by connecting cell-cell neighbors, while neglecting the actual length of the cell-cell interfaces. In Figure 9, the results of these simulations with the original parameters and the comparison with the simulations with a constant number of VSMCs through the circumferential direction are reported. We can observe that, in these simulations, some

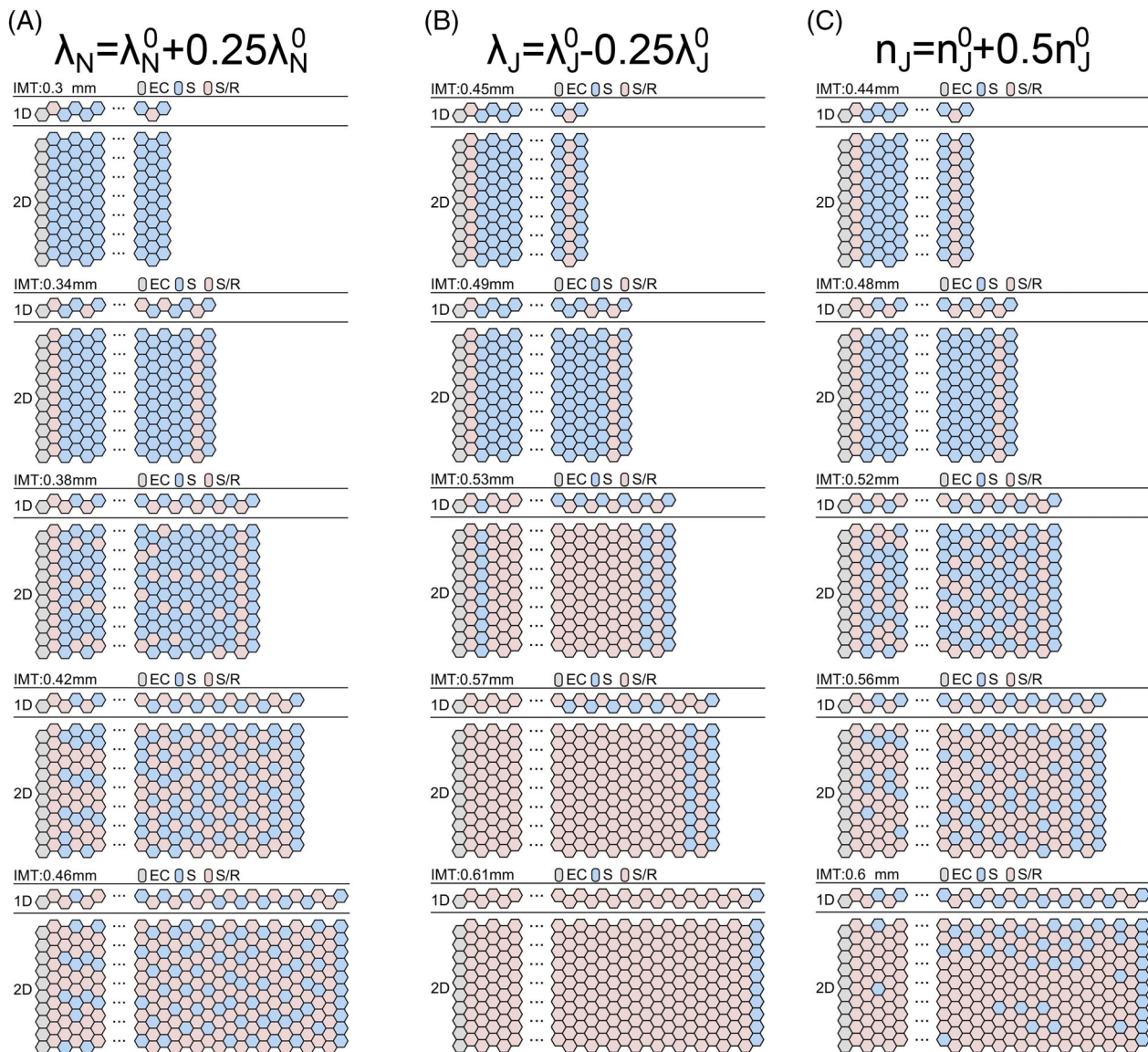


FIGURE 8 Some of the parameter sets cause a weakening of the Jagged-Notch lateral induction process and large differences between 1D and 2D simulations. Results of the simulations for representative initial conditions, for values close to the transition thickness, and for the parameter variations that were causing major differences between 1D and 2D simulations. These variations can disrupt the process of Jagged-Notch lateral induction and induce a heterogeneous distribution of Vascular Smooth Muscle Cells in terms of their phenotype both in 1D and 2D (A and C) or just in case of 1D simulations (B)

of the VSMCs do not retain the same phenotype as the surrounding neighbors (Figure 9A). This causes the phenotypic switch from synthetic to contractile VSMCs to be slightly more gradual (Figure 9B). The fact that the average values of Notch proteins and NICD are unchanged compared to simulations with a constant number of cells through the circumferential direction (Figure 9C-F) indicates that variations of NICD levels of some of the VSMCs compensate each other. This means that, when looking for example at the results for the IMT equal to 0.48 mm (Figure 9A), while a few VSMCs have relatively large values of NICD and are thus contractile, this is compensated by low values of NICD of some of the neighboring cells. As shown in Figure 9A, the VSMCs having different NICD values compared to the neighbors are located at the boundaries, where the number of cells through the circumferential direction was increased. When this cell number is increased, cells do not always have six neighbors (because of the different number of cells in different layers). Cells with a lower number of neighbors are generally in contact with a lower amount of Notch ligands, which affects their NICD level and phenotype. A similar mechanism occurs for cells with a higher number of neighbors compared to the typical number of cell neighbors, although with an opposite effect. In particular, these cells are strongly

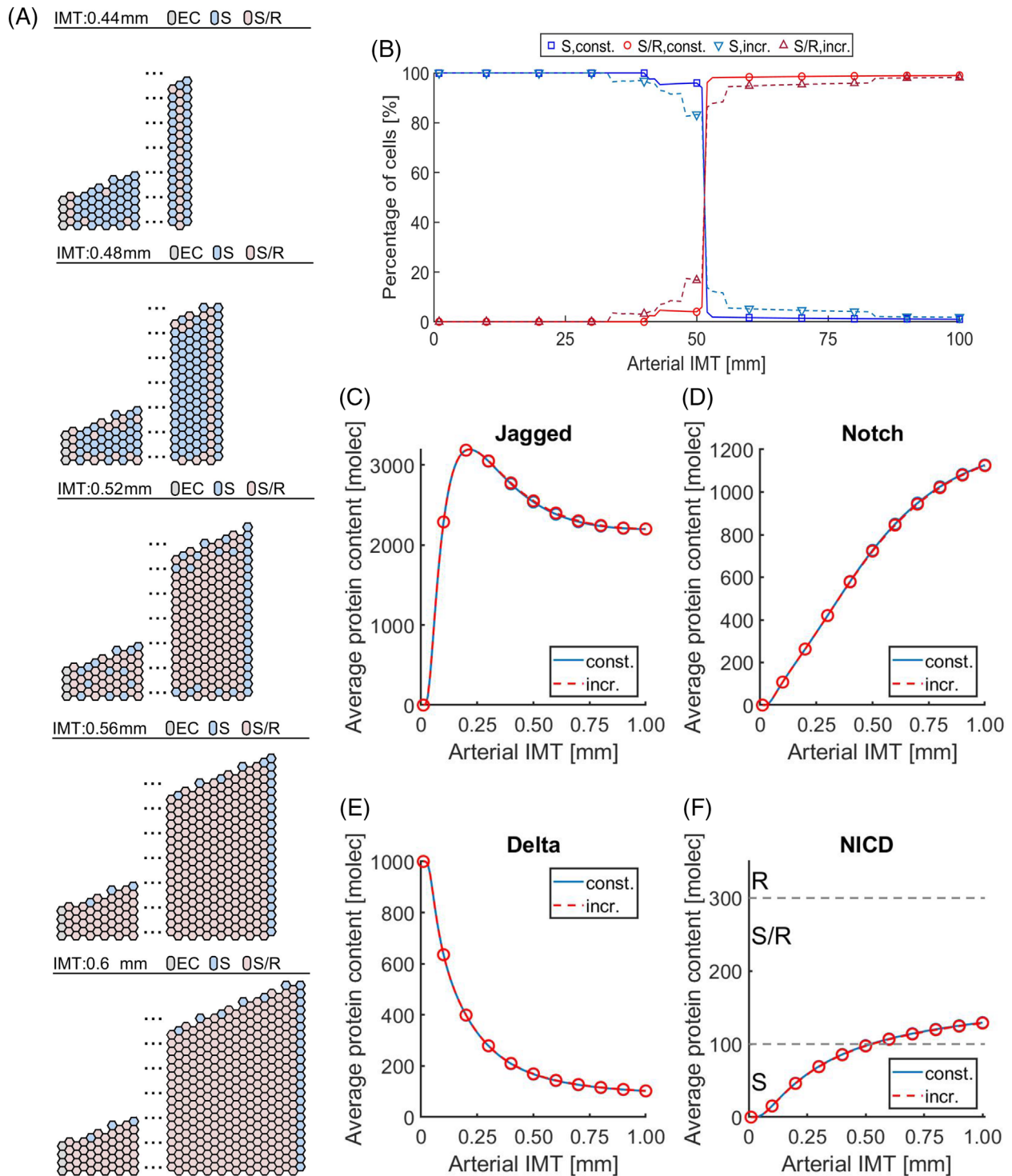


FIGURE 9 For simulations with increasing number of cells in the arterial circumferential direction, with periodic boundary conditions, some of the cells exhibit different phenotypes compared to the neighboring cells (A). This causes the Vascular Smooth Muscle Cell (VSMC) phenotypic switch to be more gradual compared to simulations with a constant number of VSMCs along the circumferential layers (B), although the switch still occurs at the same intima-media thickness (IMT) (approximately 0.50 mm). C-F) The simulations with an increasing (red) and constant (blue) number of VSMCs along the circumferential layer predict the same average values of Notch proteins for arteries of different IMT

induced to become contractile. In conclusion, the variation of cell connectivity for a few cells alters the process of Jagged-Notch lateral induction, such that the cell phenotype and the level of NICD is not completely uniform. However, the effects are very local, and only the cells with a different number of neighbors are affected. This suggests that local variations on the number of neighbors can occur without disrupting tissue homeostasis.

4 | DISCUSSION

In this study, we extended a previously developed 1D agent-based model for Notch signaling in arteries to a 2D formulation, thereby enabling the investigation of the Notch signaling dynamics for arteries having different numbers of cell neighbors and a more realistic cell distribution. The computational results indicate that, as long as periodic boundary conditions are present (such as in arteries), the number of neighbors has little effect on the predicted phenotype of VSMCs. The sensitivity analysis performed within this study indicates that this is most likely due to the presence of Jagged-Notch lateral induction, which ensures a uniform level of NICD within the entire arterial wall, dependent upon the arterial wall thickness and independent from the number of neighbors. Parameter variations weakening the Jagged-Notch lateral induction corresponded to large differences between results obtained with arteries populated by VSMCs having different cell connectivity (Figure 5). The sensitivity analysis showed that Jagged-Notch lateral induction is weakened when Notch is much more upregulated than Jagged. This highlights the importance, for future studies, to determine the effects of Notch transactivation on the Notch expression not only qualitatively but also quantitatively, as different degrees of Notch upregulation can lead to different Notch signaling dynamics.

In most of our simulations, we assumed a homogeneous distribution of cells and therefore a uniform number of cellular neighbors. When assuming that the number of cells increases from the inner to the outer layer of the arterial wall, the simulations predicted that a few VSMCs retain a different phenotype compared to the surrounding cells (Figure 9). This heterogeneity of VSMC phenotype within the same arterial wall has been observed also experimentally by Christen et al.²⁹ who observed that healthy and fully developed arterial walls are mostly populated by contractile VSMCs, but also contain a few synthetic VSMCs. As mentioned in Christen et al.,²⁹ this heterogeneity might be caused by genetic differences among VSMCs within the same population. Nevertheless, the influence of local variations in the numbers of neighbors might also contribute to the emergence of this phenotypic heterogeneity, as indicated by our simulations (Figure 9). To investigate this aspect of Notch signaling in arteries further, simulations with a more heterogeneous cellular distribution might be performed, for example, by adopting a similar approach as in Nolan and Lally,^{30,31} who investigated arterial remodeling with a 2D agent-based modeling approach considering a heterogeneous distribution of cells. Nevertheless, our simulations suggest that, although the number of cell neighbors has some very local effect on the VSMC phenotype, Notch signaling and its implications for arterial homeostasis are hardly affected in the majority of the arterial wall (Figure 9B).

The strong similarities between the 1D and 2D results for parameters associated with VSMCs in arteries corroborates the validity of the computational results from Loerakker et al.²⁰ where, with the 1D version of the agent-based model herein extended, we gave a potential explanation for the emergence and stabilization of a homeostatic arterial wall thickness. Given the similarity between 1D and 2D results and the limited computational time of 1D simulations compared to 2D, which was generally almost four times slower, the 1D approach could be adopted in future studies on Notch signaling in the arterial wall. Nevertheless, the results of the sensitivity analysis (Figure 5) indicate that the 1D simulations should be adopted only when the Jagged-Notch lateral induction process is expected to have a prominent role. Processes other than lateral induction (upregulation of Notch proteins) or inhibition (downregulation of Notch proteins) as a result of Notch transactivation can also play a role in the regulation of cellular phenotypic patterns. For example, by combining experimental and computational techniques, Sprinzak et al (2010) demonstrated that cis-inhibition of proteins within the same cell can lead to salt-and-pepper patterns without the presence of transcriptional effects of Notch transactivation. Cis-inhibition is most likely also partly responsible for the salt-and-pepper pattern that arises in the simulations shown in Figure 8A; in fact, if the same parameters are adopted while diminishing the rate of cis-inhibition k_c , the salt-and-pepper pattern is lost and the 1D simulations become again very similar to the 2D simulations (Figure S1A,B in the Supplementary Information). This suggests that, with the parameter modifications of the simulations of Figure 8A, Notch upregulation was misbalanced compared to Jagged upregulation and consequently, cells with high NICD content were prone to increase Notch more than Jagged as a result of Notch transactivation. Due to cis-inhibition, these cells degrade most of their ligands with the widely available Notch receptors and, therefore, are not able to transactivate the neighboring cells while they can still receive signal via the remaining Notch receptors. Therefore, this process can create a salt-and-pepper pattern even in case of lateral induction, which then needs to be balanced enough to counteract the effects of cis-inhibition. Cis-inhibition has been proven to occur among Notch1 and Dll1 while, to our knowledge, it still needs to be observed among Notch3 and Jagged1 VSMCs. Verifying such mechanism would be very relevant in future experimental studies, as the absence of cis-inhibition among Jagged1 and Notch3 in VSMCs might be an added control stabilizing the process and effects of lateral induction in VSMCs.

To maintain the tractability of the computational simulations and limit the computational costs, in the present study, we restricted our analysis to 2D simulations, although the proposed computational model can also be applied to 3D settings. In particular, Equations (1) to (4) proposed to describe Notch signaling for cells having different cell connectivity are general and applicable to 3D settings. For example, arterial cells and cell neighbors in the direction of the arterial length could also be considered and simulated, while assuming that the simulated artery is long enough to consider periodic boundary conditions of the system along such direction. Similar to the 2D setting (see Figures 2–4), in this case the presence of periodic boundary conditions and the process of lateral induction cause cells to have a uniform phenotype and the 3D simulations to be again equivalent to the 1D simulations, as shown in Figure S1C of the Supplementary Information. In particular, in Figure S1C we show that 1D simulations are equivalent to 3D simulations obtained by assuming that each VSMC has two neighbors for each of the three dimensions (for a total of six neighbours). This suggests not only that the proposed model can be applied to 3D but also that the findings of this study are valid also for cellular networks in 3D arteries.

The equations that were identified to extend the 1D agent-based model to a 2D formulation were obtained as a generalization of the equations proposed in Loerakker et al.²⁰ and as a more specific case compared to the equations proposed in Shaya et al.²⁸ In the latter study, Notch signaling among epithelial cells was investigated with a computational model accounting for the heterogeneity of the contact area of a single cell with its different neighbors. By comparing the computational results with experiments, they concluded that the Notch-Delta interaction between two neighbors is proportional to the length of the neighbor contact. In the present study, for simplicity, we assumed all neighbor contacts to have a constant length within the same VSMC population, thereby neglecting this potential feature of Notch signaling among VSMCs. This assumption is motivated by the fact that it is not yet clear whether Notch signaling among VSMCs occurs via filopodia or larger cell-cell contacts. Future studies might elucidate this aspect and investigate the effect of heterogeneous values of neighbor contact lengths on Notch signaling in VSMC populations.

Both here and in Loerakker et al.,²⁰ the strain experienced by VSMCs in arteries was only approximated (Equation [7] for more details) by assuming this strain to be transmurally uniform in the arterial wall. Previous studies indeed indicate that a uniform strain within arteries is ensured by residual stress.^{32,33} However, this might not be the case for arteries undergoing prolonged hypertension, which is known to cause variations of the pre-stress distribution.^{2,4,34} Furthermore, tissue-engineered arteries are expected not to exhibit residual stress right upon implantation, with a consequent heterogeneity of the strain throughout the thickness of the arterial wall. To investigate the effects of a transmurally heterogeneous strain, the present agent-based model could be coupled with a macroscopic mechanical analysis of the arterial wall, as previously done in other studies with different agent-based models.^{30,31,35,36}

In conclusion, in this study, we developed a 2D agent-based model for Notch signaling among VSMCs in arterial walls, enabling the simulation of Notch dynamics with a more physiologically representative distribution of cells. The main features of the model were tested by simulating arteries with homogeneously distributed cells. The computational simulations with the original parameter values and the sensitivity analysis suggest that cell connectivity has marginal effects on Notch dynamics in arteries when Jagged-Notch has a dominant role, while different degrees of cell connectivity lead to different outcomes when Jagged-Notch lateral induction is disrupted. This disruption process can occur when Notch is much more upregulated than Jagged as a result of Notch transactivation. Therefore, future experimental studies should focus on determining the effects of Notch transactivation not only qualitatively, but also quantitatively.

ACKNOWLEDGEMENTS

This project has been supported by the Academy of Finland (project number 218062), and it has received funding from the European Research Council (ERC) under the European Union's Horizon 2020 research and innovation program, grant agreement no. 771168 (CoG ForceMorph) and grant agreement no. 802967 (StG MechanoSignaling).

ORCID

Tommaso Ristori  <https://orcid.org/0000-0002-2800-0067>

REFERENCES

1. Wolinski H. Long-term effects of hypertension on the rat aortic wall and their relation to concurrent aging changes. *Circ Res.* 1972;30:301-309.
2. Fung YC, Liu SQ. Change of residual strains in arteries due to hypertrophy caused by aortic constriction. *Circ Res.* 1989;65(5):1340-1349.
3. Liu SQ, Fung YC. Relationship between hypertension, hypertrophy, and opening angle of zero-stress state of arteries following aortic constriction. *J Biomech Eng.* 1989;111(4):325-335.

4. Matsumoto T, Hayashi K. Stress and strain distribution in hypertensive and normotensive rat aorta considering residual strain. *J Biomech Eng.* 1996;118(1):62-73.
5. Driessen NJB, Wilson W, Bouten CVC, Baaijens FPT. A computational model for collagen fibre remodelling in the arterial wall. *J Theor Biol.* 2018;226(1):53-64.
6. Gaul RT, Nolan DR, Ristori T, Bouten CVC, Loerakker S, Lally C. Strain mediated enzymatic degradation of arterial tissue: insights into the role of the non-collagenous tissue matrix and collagen crimp. *Acta Biomater.* 2018;77:301-310.
7. Humphrey JD. Vascular adaptation and mechanical homeostasis at tissue, cellular, and sub-cellular levels. *Cell Biochem Biophys.* 2008; 50:53-78.
8. Rensen SSM, Doevendans PAFM, van Eys GJJM. Regulation and characteristics of vascular smooth muscle cell phenotypic diversity. *Neth Heart J.* 2007;15(3):100-108.
9. Shinohara S, Shinohara S, Kihara T, Miyake J. Regulation of differentiated phenotypes of vascular smooth muscle cells. In: Sugi H, ed. *Current basic and pathological approaches to the function of muscle cells and tissues—from molecules to Humans. Rijeka, Croatia: IntechOpen;* 2012:331-344.
10. Thyberg J, Blomgren K, Hedin U, Dryjski M. Phenotypic modulation of smooth muscle cells during the formation of neointimal thickenings in the rat carotid artery after balloon injury: an electron-microscopic and stereological study. *Cell Tissue Res.* 1995;281(3):421-433.
11. Owens GK, Kumar MS, Wamhoff BR. Molecular regulation of vascular smooth muscle cell differentiation in development and disease. *Physiol Rev.* 2004;84(3):767-801.
12. Petsophonsakul P, Furmanik M, Forsythe R, et al. Role of vascular smooth muscle cell phenotypic switching and calcification in aortic aneurysm formation. *Arterioscler Thromb Vasc Biol.* 2019;39(7):1351-1368.
13. Tang Y, Urs S, Boucher J, et al. Notch and transforming growth factor-beta (TGFbeta) signaling pathways cooperatively regulate vascular smooth muscle cell differentiation. *J Biol Chem.* 2010;285(23):17556-17563.
14. Boucher J, Gridley T, Liaw L. Molecular pathways of notch signaling in vascular smooth muscle cells. *Front Physiol.* 2012;3:81.
15. Lindner V, Booth C, Prudovsky I, Small D, Maciag T, Liaw L. Members of the Jagged/Notch gene families are expressed in injured arteries and regulate cell phenotype via alterations in cell matrix and cell-cell interaction. *Am J Pathol.* 2001;159(3):875-883.
16. Collier JR, Monk NA, Maini PK, Lewis JH. Pattern formation by lateral inhibition with feedback: a mathematical model of delta-notch intercellular signalling. *J Theor Biol.* 1996;183(4):429-446.
17. Boareto M, Jolly MK, Lu M, Onuchic JN, Clementi C, Ben-Jacob E. Jagged-Delta asymmetry in Notch signaling can give rise to a sender/receiver hybrid phenotype. *Proc Natl Acad Sci U S A.* 2015;112(5):E402-E409.
18. Manderfield LJ, High FA, Engleka KA, et al. Notch activation of Jagged1 contributes to the assembly of the arterial wall. *Circulation.* 2012;125(2):314-323.
19. High FA, Zhang M, Proweller A, et al. An essential role for Notch in neural crest during cardiovascular development and smooth muscle differentiation. *J Clin Invest.* 2007;117(2):353-363.
20. Loerakker S, Stassen OMJA, Ter Huurne FM, Boareto M, Bouten CVC, Sahlgren CM. Mechanosensitivity of Jagged-Notch signaling can induce a switch-type behavior in vascular homeostasis. *Proc Natl Acad Sci U S A.* 2018;115(16):E3682-E3691.
21. Liu H, Kennard S, Lilly B. Notch3 expression is induced in mural cells through an autoregulatory loop that requires endothelial-expressed Jagged1. *Circ Res.* 2009;104(4):466-475.
22. Noseda M, Fu Y, Niessen K, et al. Smooth muscle alpha-Actin is a direct target of notch/CSL. *Circ Res.* 2006;98(12):1468-1470.
23. Morrow D, Sweeney C, Birney YA, et al. Cyclic strain inhibits Notch receptor signaling in vascular smooth muscle cells in vitro. *Circ Res.* 2005;96(5):567-575.
24. Wilson E, Mai Q, Sudhir K, Weiss RH, Ives HE. Mechanical strain induces growth of vascular smooth muscle cells via autocrine action of PDGF. *J Cell Biol.* 1993;23:741-747.
25. Birukov KG, Shirinsky VP, Stepanova OV, et al. Stretch affects phenotype and proliferation of vascular smooth muscle cells. *Mol Cell Biochem.* 1995;144(2):131-139.
26. Reusch P, Wagdy H, Reusch R, Wilson E, Ives HE. Mechanical strain increases smooth muscle and decreases nonmuscle myosin expression in rat vascular smooth muscle cells. *Circ Res.* 1996;79(5):1046-1053.
27. Sprinzak D, Lakhnpal A, Lebon L, et al. Cis-interactions between Notch and Delta generate mutually exclusive signalling states. *Nature.* 2010;465(7294):86-90.
28. Shaya O, Binshtok U, Hersch M, et al. Cell-cell contact area affects Notch signaling and Notch-dependent patterning. *Dev Cell.* 2017;40 (5):505-511.e6.
29. Christen T, Bochaton-Piallat ML, Neuville P, et al. Cultured porcine coronary artery smooth muscle cells. A new model with advanced differentiation. *Circ Res.* 1999;85(1):99-107.
30. Nolan DR, Lally C. Coupled finite element agent-based models for the simulation of vascular growth and remodeling. In: Cerrolaza M, Shefelbine S, Garzón-Alvarado D, eds. *Numerical Methods and Advanced Simulation in Biomechanics and Biological Processes. Cambridge, Massachusetts: Academic Press;* 2017:283-300.
31. Nolan DR, Lally C. An investigation of damage mechanisms in mechanobiological models of in-stent restenosis. *J Comput Sci.* 2018;24: 132-142.
32. Chuong CJ, Fung YC. On residual stresses in arteries. *J Biomech Eng.* 1986;108(2):189-192.
33. Destrade M, Liu Y, Murphy JG, Kassab GS. Uniform transmural strain in pre-stressed arteries occurs at physiological pressure. *J Theor Biol.* 2012;303:93-97.

34. Fung YC, Liu SQ. Changes of zero-stress state of rat pulmonary arteries in hypoxic hypertension. *J Appl Physiol*. 1991;70(6):2455-2470.
35. Thorne BC, Hayenga HN, Humphrey JD, Peirce SM. Toward a multi-scale computational model of arterial adaptation in hypertension: verification of a multi-cell agent based model. *Front Physiol*. 2011;2:20.
36. Zahedmanesh H, Lally C. A multiscale mechanobiological modelling framework using agent-based models and finite element analysis: application to vascular tissue engineering. *Biomech Model Mechanobiol*. 2012;11(3-4):363-377.
37. Amsen D, Blander JM, Lee GR, Tanigaki K, Honjo T, Flavell RA. Instruction of distinct CD4 T helper cell fates by different notch ligands on antigen-presenting cells. *Cell*. 2004;117(4):515-526.
38. Wang MM. Notch signaling and Notch signaling modifiers. *Int J Biochem Cell Biol*. 2011;43(11):1550-1562.
39. Brabletz S, Bajdak K, Meidhof S, et al. The ZEB1/miR-200 feedback loop controls Notch signalling in cancer cells. *EMBO J*. 2011;30(4):770-782.
40. Gill JG, Langer EM, Lindsley RC, et al. Snail and the microRNA-200 family act in opposition to regulate epithelial-to-mesenchymal transition and germ layer fate restriction in differentiating ESCs. *Stem Cells*. 2011;29(5):764-776.
41. Timmerman LA, Grego-Bessa J, Raya A, et al. Notch promotes epithelial-mesenchymal transition during cardiac development and oncogenic transformation. *Genes Dev*. 2004;18(1):99-115.
42. Bjällmark A, Lind B, Peolsson M, Shahgaldi K, Brodin LA, Nowak J. Ultrasonographic strain imaging is superior to conventional non-invasive measures of vascular stiffness in the detection of age-dependent differences in the mechanical properties of the common carotid artery. *Eur J Echocardiogr*. 2010;11(7):630-636.
43. Yuda S, Kaneko R, Muranaka A, et al. Quantitative measurement of circumferential carotid arterial strain by two-dimensional speckle tracking imaging in healthy subject. *Echocardiography*. 2011;28(8):899-906.
44. Tanaka H, Dinunno FA, Monahan KD, DeSouza CA, Seals DR. Carotid artery wall hypertrophy with age is related to local systolic blood pressure in healthy men. *Arterioscler Thromb Vasc Biol*. 2001;21(1):82-87.
45. Bianchini E, Bozec E, Gemignani V, et al. Assessment of carotid stiffness and intima-media thickness from ultrasound data: comparison between two methods. *J Ultrasound Med*. 2010;29(8):1169-1175.
46. van den Munckhof I, Scholten R, Cable NT, Hopman MT, Green DJ, Thijssen DH. Impact of age and sex on carotid and peripheral arterial wall thickness in humans. *Acta Physiol (Oxf)*. 2012;206(4):220-228.

SUPPORTING INFORMATION

Additional supporting information may be found online in the Supporting Information section at the end of this article.

How to cite this article: Ristori T, Stassen OMJA, Sahlgren CM, Loerakker S. Lateral induction limits the impact of cell connectivity on Notch signaling in arterial walls. *Int J Numer Meth Biomed Engng*. 2020;36:e3323. <https://doi.org/10.1002/cnm.3323>

APPENDIX

Derivation of Equations (1) to (4)

In the present study, we extended the 1D model of Loerakker et al.²⁰ to a 2D formulation. The differential equations describing the time evolution of the Notch proteins in VSMCs were obtained as a less general approach of equations proposed in Shaya et al.,²⁸ and as a generalization of the approach taken in Loerakker et al.²⁰ In what follows, we describe the procedure to obtain the ordinary differential equation describing the time variation of Notch, N_{ij} . A similar procedure can be followed for J_{ij} , D_{ij} , and I_{ij} .

Similar to Shaya et al.,²⁸ instead of considering immediately the total quantity of Notch proteins in a cell, we start by modeling the density of Notch ligands. For simplicity of notation, in what follows we indicate with h the cell ij , such that $n_{h,k}$ is the density of Notch ligands present on the membrane of cell h , at the interface with the single cell neighbor k . $d_{h,k}$ and $j_{h,k}$ represent analogous quantities for Delta and Jagged. On the other hand, $d_{k,h}$ and $j_{k,h}$ are the density of Delta and Jagged present on the membrane of the cell k , at the interface with the cell neighbor h . Thus, these two quantities represent the Notch ligands available for binding with the Notch receptor $n_{h,k}$. The time variation of the density of Notch receptors can be modeled by

$$\frac{dn_{h,k}}{dt} = \frac{N_{pr,mech} H^S}{L_h} - \hat{k}_c n_{h,k} (d_{h,k} + j_{h,k}) - \hat{k}_t (d_{k,h} + j_{k,h}) - \gamma n_{h,k}, \quad (A1)$$

where, for simplicity of notation, we have neglected the variables of the function H^s . The first term on the right-hand side describes the production of Notch which is distributed isotropically over the perimeter of the cell L_h . The second term describes the cis-inhibition of Notch receptors with Notch ligands within the same cell. The third term represents the transactivation of Notch receptors in the cell h by Notch ligands in the cell k . The last term represents the degradation of Notch receptors within the cell h .

We observe that the parameters \hat{k}_c and \hat{k}_t are not exactly the same as the parameters k_c and k_t adopted in Boareto et al.¹⁷ and Loerakker et al.²⁰ In fact, while the dimension of k_c and k_t is [molecules⁻¹s⁻¹], the dimension of \hat{k}_c and \hat{k}_t is [m¹molecules⁻¹s⁻¹]. The parameters k_c and k_t will be obtained from \hat{k}_c and \hat{k}_t , respectively, via a normalization procedure.

The density of Notch ligands $n_{h,k}$ is related to the total amount of Notch ligands $N_h = \sum_{k=1}^{M_h} n_{h,k} l_{h,k}$, where M_h is the number of neighbors of cell h , and $l_{h,k}$ is the length of the interface between cell h and cell k . Given this relationship, we can find the time variation of the total amount of Notch receptors:

$$\frac{dN_h}{dt} = \frac{d}{dt} \sum_{k=1}^{M_h} l_{h,k} n_{h,k} = \sum_{k=1}^{M_h} l_{h,k} \frac{dn_{h,k}}{dt} = \quad (\text{A2})$$

$$= N_{\text{pr,mech}} H^s \frac{\sum_{k=1}^{M_h} l_{h,k}}{L_h} - \hat{k}_c \sum_{k=1}^{M_h} l_{h,k} n_{h,k} (d_{h,k} + j_{h,k}) - \hat{k}_t \sum_{k=1}^{M_h} l_{h,k} n_{h,k} (d_{k,h} + j_{k,h}) - \gamma \sum_{k=1}^{M_h} l_{h,k} n_{h,k} = \quad (\text{A3})$$

$$= N_{\text{pr,mech}} H^s - \hat{k}_c \sum_{k=1}^{M_h} l_{h,k} n_{h,k} (d_{h,k} + j_{h,k}) - \hat{k}_t \sum_{k=1}^{M_h} l_{h,k} n_{h,k} (d_{k,h} + j_{k,h}) - \gamma N_h. \quad (\text{A4})$$

By assuming that the rate of diffusion of Notch proteins within the cell membrane is much larger than the rate of Notch protein binding, production, and degradation, we have that $n_{h,k} = n_{h,k'}$ for all k, k' neighbors of the cell h , and thus $N_h = n_{h,k} L_h$. Similarly, $D_h = d_{h,k} L_h$ and $J_h = j_{h,k} L_h$. From this, Equation (A4) becomes

$$\frac{dN_h}{dt} = N_{\text{pr,mech}} H^s - \hat{k}_c \frac{N_h}{L_h} (D_h + J_h) - \hat{k}_t \frac{N_h}{L_h} \sum_{k=1}^{M_h} l_{h,k} (d_{k,h} + j_{k,h}) - \gamma N_h.$$

At this point, for simplicity we assume that the length of the interface between each cell neighbor in a single population is equal to a constant value l . This assumption is here motivated by the fact that it is not yet clear whether VSMCs interact with Notch signaling via filopodia, lamellipodia, or larger cell-cell contacts. From this, it follows that $l_{h,k}$ does not depend on h and k , and Equation (A5) becomes

$$\frac{dN_h}{dt} = N_{\text{pr,mech}} H^s - \hat{k}_c \frac{N_h}{L_h} (D_h + J_h) - \hat{k}_t \frac{N_h}{L_h} \sum_{k=1}^{M_h} \frac{D_k + J_k}{M_k} - \gamma N_h,$$

where M_k is the number of cell neighbors of the cell neighbor k . Now we normalize \hat{k}_c and \hat{k}_t with the average perimeter of VSMCs L , assuming that this average is constant among different cell populations; we define $k_c = \frac{\hat{k}_c}{L}$ and $k_t = \frac{\hat{k}_t}{L}$, which are equivalent to the parameters adopted in the main text (with the same dimension). Given this definition, we have

$$\frac{dN_h}{dt} = N_{\text{pr,mech}} H^s - k_c \frac{L}{L_h} N_h (D_h + J_h) - k_t \frac{L}{L_h} N_h \sum_{k=1}^{M_h} \frac{D_k + J_k}{M_k} - \gamma N_h.$$

Finally, by introducing M as the average number of cell neighbors and l as the length of each cell-cell contact within a single cell population, we have $L = Ml$ and $L_h = M_h l$, such that:

$$\frac{dN_h}{dt} = N_{\text{pr,mech}} H^s - k_c \frac{M}{M_h} N_h (D_h + J_h) - k_t \frac{M}{M_h} N_h \sum_{k=1}^{M_h} \frac{D_k + J_k}{M_k} - \gamma N_h. \quad (\text{A5})$$

which is the equation reported in the main text.

We here observe that, when VSMCs within a population have constantly the same number of neighbors, then $M_k = M_{k'}$ for each k, k' cell neighbor and $L = L_h = LM_h$ for each VSMC h . In that case, Equation (A5) becomes

$$\frac{dN_h}{dt} = N_{\text{pr,mech}} H^s - k_c N_h (D_h + J_h) - k_t \frac{N_h}{M_h} \sum_{k=1}^{M_h} (D_k + J_k) - \gamma N_h. \quad (\text{A6})$$

When $M_h = 2$ this equation is equivalent to the approach adopted in Boareto et al.¹⁷ and Loerakker et al.²⁰

Parameter values motivated by experiments

The model parameters for the computational simulations were chosen as in our previous work,²⁰ and similar to the previous study of Boareto et al.¹⁷ As such, the choice of the parameters can be justified on the same grounds, which we summarize here, approximately following the order of the parameters as reported in Table 1. The values of Notch and Jagged production rates (N_{pr} and J_{pr}) were chosen so that the model predicts that each cell contains a few thousands of proteins as a maximum value, as experimentally motivated.^{17,37} In a similar fashion, the value of I_0 was chosen to reflect the fact that the value of NICD within the nucleus is usually in the order of a few hundred.¹⁷ Since no Delta protein expression was reported for VSMCs in vivo¹⁹ and little expression was observed in vitro,²⁰ a small value for the Delta production rate (D_{pr}) was chosen, such that $J_{\text{pr}} \gg D_{\text{pr}}$. The Jagged protein content in endothelial cells (J_{EC}) was then chosen approximately equal to the value of J that had been predicted across cells in arteries without mechanical stimuli. As experimentally motivated,²⁷ the cis-inhibition rate (k_c) was assumed to be one order of magnitude higher than the transactivation rate (k_t). As Notch signaling is known to decay quite quickly,³⁸ the degradation of NICD (γ_I) was chosen five times faster than the degradation of other Notch proteins (γ). Although other cross-talking pathways might be involved, Delta-Notch signaling often mediates lateral inhibition processes and, therefore, Notch transactivation has often been assumed to downregulate Delta expression,^{16,17} which entails $\lambda_D < 1$. On the other hand, as shown experimentally (see supplementary material of our previous work²⁰), Notch transactivation by external Jagged proteins upregulates the production of Jagged1 and Notch3, and thus λ_J and λ_N were chosen accordingly ($\lambda_J > 1$, $\lambda_N > 1$). As in Boareto et al.,¹⁷ the values of the Hill coefficients n_N and n_D were based on the experimental data fitting performed by Sprinzak et al.,²⁷ while a higher value for n_J was chosen to account for Notch crosstalking pathways via miR200 and Snail.³⁹⁻⁴¹ The sensitivity of Notch3 and Jagged1 production to strain (A_N and A_J) were based on the experimental data fitting that we performed in our previous study.²⁰ The average physiological strain (ε_p) and the radius (r) of native human carotid arteries were based on experimental data from the literature.⁴²⁻⁴⁶ Finally, the average physiological stress (σ_p) was estimated with the Laplace's equation, starting from the physiological systolic pressure (p) and IMT values reported in the literature.⁴³⁻⁴⁶